GEOMETRICAL INSTABILITIES IN ASYMMETRIC PLATES REINFORCED WITH 3D INTERLOCK FABRICS

Benavente, M.[1], Courtois, A.[1], Marcin, L.[2], Godon, T.[3] Levesque, M. [1]
and Ruiz, E. [1*]
[1] Mechanical engineering, École Polytechnique, Montreal, Canada
[2] SAFRAN TECH, Chateaufort, France
[3]SAFRAN AIRCRAFT ENGINES, Moissy-Cramayel, France

* Corresponding author (edu.ruiz@polymtl.ca)

Keywords: *Fiber-reinforced Composites, Process Modelling, Liquid Composites Molding*

ABSTRACT

Over the last decades the factors leading to the development of residual stresses during the manufacturing of laminated composites materials have been studied, both experimentally and numerically since the presence of residual stresses can generate geometrical instabilities and/or modify the mechanical performance of the part. In the present work the geometrical instabilities of asymmetric composite plates reinforced with three-dimensional (3D) fabrics and manufactured by Resin Transfer Moulding (RTM) have been studied using a Digital Image Analysis system. Laminates consisting of two ply were manufactured using 3D woven interlock fabrics with carbon fiber from Hexcel and a Diglycidyl Ether of Bisphenol F (DGEBF) epoxy resin. The plate's deformation were monitored after the fabrication and during a free-standing isotherm near the resins ultimate glass transition temperature. Finally, a finite element model has been developed to simulate the residual stresses generated during the cool-down stage. A comparison between an elastic model and a viscoelastic model for the geometrical instability prediction is also presented in this work. This study aims to better understand the geometrical instabilities induce in composite parts reinforced with 3D interlock fabrics during RTM manufacturing and how they evolve with temperature and time.

1 INTRODUCTION

Thermoset composites have been increasingly used in aerospace applications over the last 60 years. This trend is partially due to their high specific mechanical properties (stiffness-to-weight ratio), capability of high degree of optimization and outstanding fatigue and corrosion resistance. However, their low impact damage and delamination resistance and post manufacturing geometrical instability have limited their implementation. 3D woven fabric architectures are being developed to overcome the mechanical limitations encountered with two-dimensional laminates [1, 2]. 3D interlock reinforcements are composed by superposed weft tows that are linked in-plane and out-of-plane by warp tows, as shown in Figure 1-1 .The presence of tows in the through thickness direction improve the impact damage and delamination resistance while reducing the molding costs for thick parts when compared to two-dimensional (2D) laminates [1].

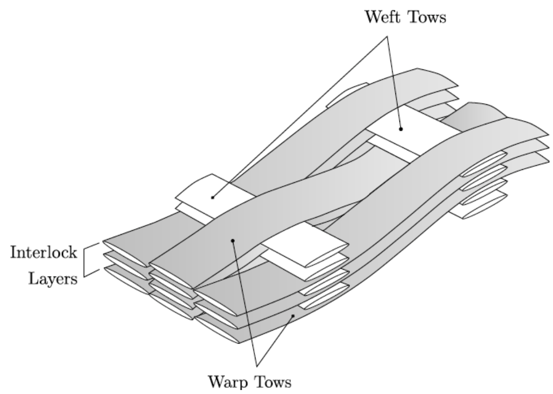

Figure 1-1. Schematic representation of a 3D interlock ply with four interlock layers.

Geometrical instabilities in composite parts are caused by the presence of residual stresses developed during its manufacturing process or at the post-curing. The chemical shrinkage suffered by the resin during curing, the thermal expansion mismatch between the reinforcement and the matrix and the tool-part interaction are known to be the main causes of the residual stresses generation [3-5]. Linear Variable Differential Transducer (LVDT) sensor [6], Fibber Bragg Grating (FBG) [7, 8] and digital image correlation analysis [9-11] have been used, among others, to study the geometrical instabilities of plates caused by the residual stresses.

Some authors observed an increment of the plate's total deformation after having set the plate to an isotherm above the resin's ultimate glass transition temperature [4, 12]. Svanberg and Holmberg introduced the term "frozen-in deformation" which is related to the constrains imposed by the mold during manufacturing. These "frozen-in deformations" are released when the part is reheated freestanding above the glass transition temperature, thus increasing the total deformation of the part when it is cooled-down to room temperature.

In the present work the physical origins of process-induced residual distortions in asymmetric plates reinforced with 3D woven interlock fabric have been studied. Digital image correlation system has been used to measure the geometrical instabilities after the manufacturing and their evolution during a 150 minutes isotherm below the glass transition temperature. Finally, a thermo-viscoelastic model has been implemented into a commercial finite element software (ABAQUS) to simulate the residual stresses development. These numerical results are finally compared with a thermo-elastic simulation model and the experimental results.

2 EXPERIMENTAL METHODOLOGY

2.1 Plates manufacturing

Each 3D woven ply used in this work was composed of four interlock layers, thus there were four stacked tows through the thickness direction. The reinforcement has a 70/30 warp/weft ratio, meaning that 70% of the fibers mass is distributed along the warp direction. A commercial Diglycidyl Ether of Bisphenol F (DGEBF) one component epoxy resin was used as the matrix [13]. Longitudinal injections were carried out in a rectangular steel mold with an internal cavity of 455 x 145 x 6.7 mm to manufacture carbon/epoxy laminates with 58% fiber volume fraction. Two plies, one of them with the warp tows oriented along the longitudinal direction and the other along the transversal direction were stacked to obtain a [0/90] lay-up configuration. Three micro thermocouples were embedded into the reinforcement, in the center of the mold at the bottom and top surfaces, and between the two plies. Once the preform was draped, the mold was closed and preheated at ultimate Tg of the resin. The epoxy system was heated above 100°C to reduce its viscosity and degassed for 30 minutes prior to the injection to minimize the risks of porosity. Resin was then injected at a constant flow rate of 20 ml/min followed by a compaction pressure of 7 bars to reduce the porosity generation during resin polymerization [13]. A cure cycle with two dwells, one hour at Tg followed by two hours at Tg+20°C was used to ensure full resin curing. The plate was then cooled-down inside the mold, and when the center of the laminate reached 100°C the plate was released from the mold and cooled-down by natural convection to room temperature. A total of five plates were manufactured under same conditions to account for process variabilities.

2.2 Characterization of geometrical instabilities

Digital image correlation analysis was used to measure the plate's geometrical instabilities after manufacturing. A high-resolution digital camera from Point Grey was set to acquire images with a resolution of 2448 x 2048 pixels. The camera was aligned horizontally with the sample, capturing the whole longitudinal edge, as shown in Figure 2-1. Three lamps were used to ensure a proper lighting of the plate. The plates' longitudinal edges were painted in white and a black painted aluminum plate was used as a background to increase the images contrast. A ruler was placed besides the composite to calibrate the pixels size. Finally, a MATLAB code was developed to process the images using the least-square method to compute the plate's deflection. In addition, the plate's longitudinal deflection was measured at room temperature by an electronic LVDT. A total of forty-two measurements, one per centimeter, were taken in the middle axis of each sample. In all cases, the measurements taken with the LVDT presented a good agreement with those obtained by the digital image correlation system.

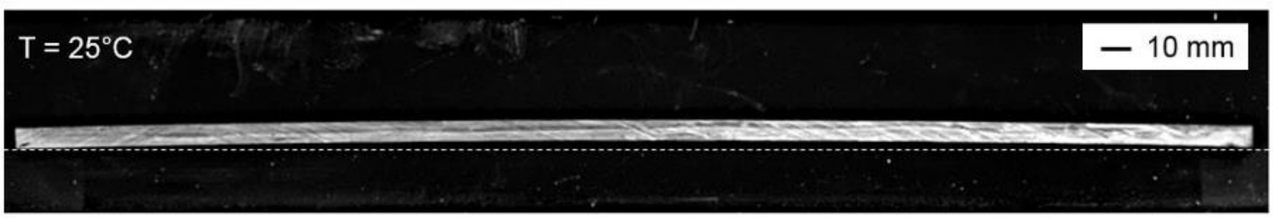

Figure 2-1. Geometrical instability at room temperature after the manufacturing of the asymmetric plate reinforced with 3D interlock reinforcement

The plates were then reheated freestanding in a convection oven during 150 minutes at Tg-10°C. The cameras were placed in front of the convection oven window, thus monitoring the warpage evolution during the experiment. After the 150 minutes isotherm the plates were removed from the oven and cooled-down by natural convection to room temperature. The total deformation of the plates at room temperature was then measured by LVDT.

3 NUMERICAL MODELLING

The geometrical evolution of composites plates after molding was studied numerically using the commercial finite element software ABAQUS. A staggered approach was implemented for this numerical calculation. First a heat transfer analysis was conducted to predict the temperature evolution through the thickness of the part. Then, a stress analysis was performed to compute the plate's geometrical evolution during the cool-down using the temperature gradient computed in the heat transfer analysis. It was assumed that the part was completely polymerized and strain-free prior to the cool-down. Therefore the molding conditions (injection and resin curing) were not considered in this simulation.

3.1 Material modelling

WiseTex software was used to simulate the geometrical model of the 3D interlock fabric. Homogenized properties as a function of time and temperature were computed using the resin's mechanical which were characterized in previous works [14].

3.1.1 Mechanical constitutive model

Two 3D orthotropic temperature dependent constitutive models have been implemented in ABAQUS using UMAT user subroutine. The increment step used for the thermo-elastic and thermo-viscoelastic solutions is presented in the section below.

The stresses tensor in the part, σ_{ij} can be expresses as a function of the total deformation, ε_{kl} as:

$$\sigma_{ij(t)} = \int_0^t C_{ijkl}\left(t-\tau, T\right) : \frac{d\varepsilon_{kl}}{d\tau} d\tau \qquad 1$$

where C_{ijkl} is the rigidity matrix, time and temperature dependent. For linearly elastic models it is assumed that the rigidity matrix remains constant through the time. Thus, the elastic increment can be expressed as

$$\sigma_{ij(t+\Delta t)} = \sigma_{ij(t)} + \Delta\sigma_{ij} \qquad 2$$

$$\Delta\sigma_{ij} = \Delta C_{ijkl}(\mathrm{T}) : \varepsilon_{kl} + C_{ijkl}(\mathrm{T}) : \Delta\varepsilon_{kl} \qquad 3$$

where the rigidity matrix is only temperature dependent

Equation 1 can be written using Prony series [14, 15] to develop the rigidity matrices C_{ijkl} for the thermo-viscoelastic approach:

$$\sigma_{ij(t)} = \int_0^t \left[C_{ijkl}^{\infty} + \sum_{n=1}^{N} C_{ijkl}^{n} \exp\left[-\frac{(\mathrm{t}-\tau)}{\omega^n} \right] : \right] \frac{d\varepsilon}{d\tau} d\tau \qquad 4$$

where C_{ijkl}^{∞} is the completely relaxed tensor and C_{ijkl}^{n} are the relaxation tensors associated to relaxation times ω^n

And N is the number of Prony series used in the solution. Machado et al.[15] presented the incremental form suitable for the finite element implementation of Eq. 1 based on the Prony series development presented in Eq. 4

$$\Delta\sigma_{ij} = C_{ijkl}^{0} : \Delta\varepsilon_{kl} - \sum_{n=1}^{N} C_{ijkl}^{n} : \Delta\varepsilon_{kl}^{n} \qquad 5$$

where C_{ijkl}^{0} is the instantaneous rigidity matrix expressed as follows:

$$C_{ijkl}^{0} = C_{ijkl}^{\infty} + \sum_{n=1}^{N} C_{ijkl}^{n} \qquad 6$$

and $\Delta\varepsilon_{kl}^{n}$ is the viscous strain increment and calculated as:

$$\Delta\varepsilon_{kl}^{n} = \frac{aT\omega_n}{\Delta t}\left(\frac{\Delta t}{\omega_n aT} + \exp\left(-\frac{\Delta t}{\omega_n aT} \right) - 1 \right)\Delta\varepsilon_{kl} + \left(1 - \exp\left(-\frac{\Delta t}{aT\omega_n} \right) \right)\left(\varepsilon_{kl(t-1)} - \varepsilon_{kl(t-1)}^{n} \right) \qquad 7$$

where aT is the temperature shift factor computed using Arrhenius (8), thus taken into account the material dependence with the temperature.

$$\log(aT) = \frac{E_a}{\ln 10 R}\left(\frac{1}{T} - \frac{1}{T_g}\right) \qquad 8$$

where E_a is the activation energy (J/mol), R is the universal gas constant (8,314 J/Kmol).

3.2 Geometry and boundary conditions

A 6.7 mm thick composite plate was modeled using the actual dimension of the manufactured composite plates. Due to the symmetry of the problem only one quarter of the plate was analyzed. The two plies were simulated as two sections of the same part with a different material orientation. Four elements were used through the composite thickness and three-dimensional 8-nodes solid elements, DC3D8 and C3D8 for the heat transfer and stress analysis, respectively, were used.

The temperature measured with the thermocouples during the plate cool-down inside of the mold was used as temperature input for the numerical analysis. The temperature field was applied to the top and the bottom of the plate. During the cool-down outside of the mold, natural convection was applied by defining 7.5 W/m^2 as the heat transfer coefficient.

In order to reproduce the model symmetry, the displacements of the nodes located on the symmetric planes XZ and YZ were fixed in the direction 1 and 2 respectively. During the cool-down inside of the mold (from 180°C to 100°C) a perfect bonding between the mold and the part was assumed. Thus, the nodes were fixed during this stage of the process to simulate the mold constraints. The rest of the process was computed by fixing the node at the bottom corner, located at the intersection of the two symmetric planes in the Z direction, thus avoiding the possible rigid motion, as shown in Figure 3-1.

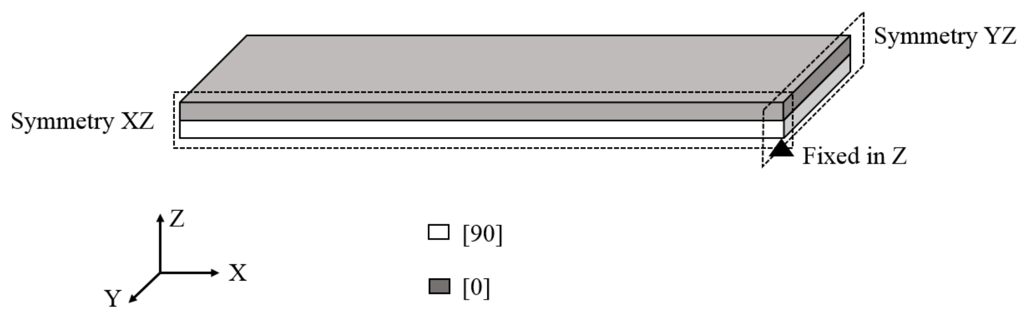

Figure 3-1 Composite plate finite element model

Finally, the isotherm at 140°C during 150 minutes was simulated with a free-standing condition, thus the plate could deform freely with time and temperature. The temperature was computed by applying a heat transfer coefficient of 20W/m^2.

A schematic representation of the temperature and boundary conditions applied to the plate during the numerical simulation are presented in Figure 3-2. During the first 50 minutes the plate was constrained by the mold, and therefore, the plate was completely fixed. Once the part was released from the mold, the part was free-standing, and therefore free to deform.

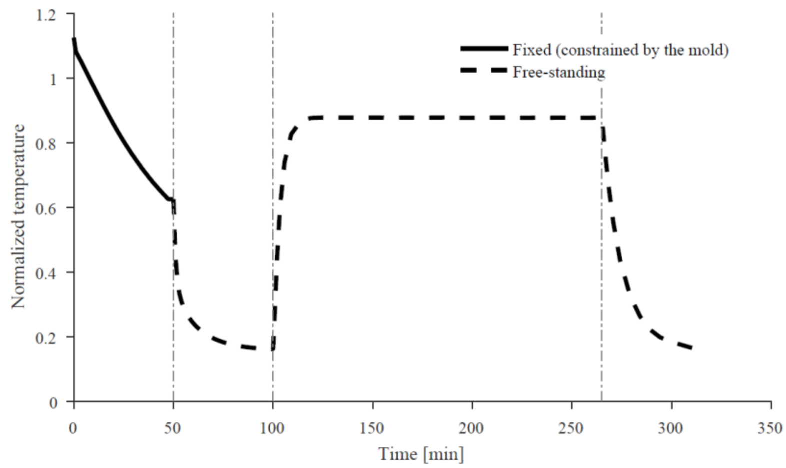

Figure 3-2. Temperature and boundary condition applied during the finite element model.

4 RESULTS AND DISCUSSION

For improved readability, all results presented in this section are normalized by the maximum value of the experimental deflection.

4.1.1 Total warpage

The longitudinal deflection obtained after the cool-down for the numerical simulations and the experimental results at room temperature are presented in Figure 4-1. The difference observed between the two models can be explained by the fact that the viscoelastic model takes into account the possible residual stresses relaxation occurred at high temperature when the plate is constrained inside the mold. The relaxation of residual stresses experienced at high temperature implies a reduction of the plate's total deformation. Experimental data fit between of those two models.

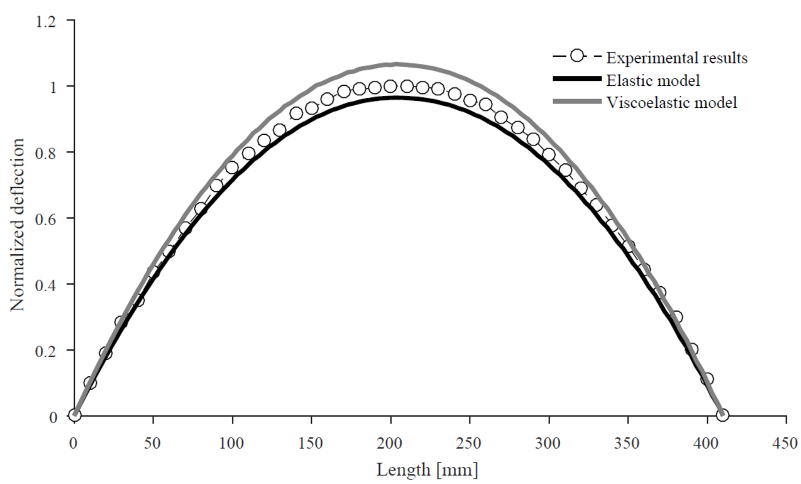

Figure 4-1. Comparison of the longitudinal deflection of asymmetric plates reinforced with 3D interlock fabric obtained experimentally and with numerical models

4.1.2 *Warpage evolution with the time and temperature*

The plate's curvature evolution was recorded using the digital image analysis during the heating and the 150 minutes isotherm. One picture per second was taken during this experimentation. The temperature evolution was monitored by the micro-thermocouples already embedded in the plate. The experimental evolution of the plate's deflection during the isotherm at Tg-20°C is presented in Figure 4-2. It is observed that the isotherm temperature was stabilized after the first 15 minutes. During this period, the deformation caused by the coefficient of thermal expansion decreases linearly with the raise in temperature (thermo-elastic deformation). Once the isotherm temperature is achieved, it was observed a 6% increment of the plate's total deflection within the 150 minutes isotherm. The deflection dependence with time at high temperature suggests that the composites experiences viscoelastic behavior (creep) at temperatures close to its glass transition temperature.

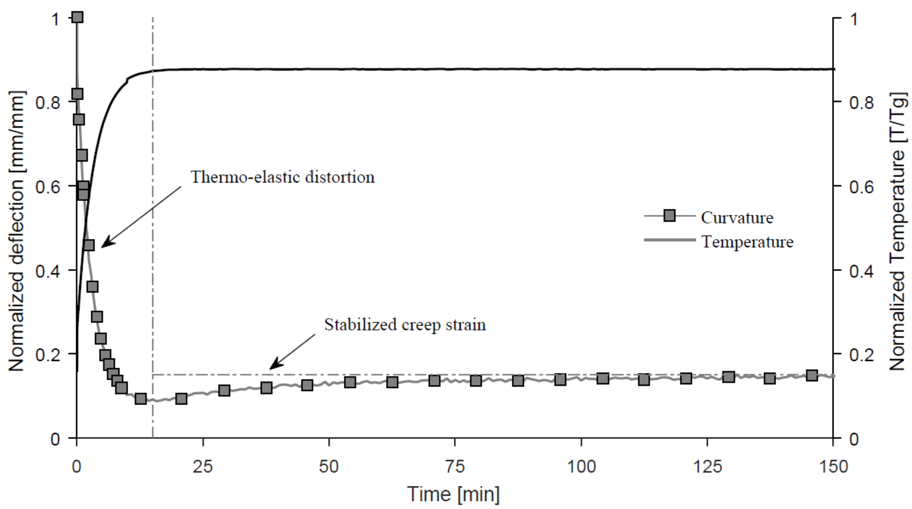

Figure 4-2. Deflection evolution of a [0/90] plate with time during the ramp isotherm at Tg-20°C.

Figure 4-3 shows the deflection evolution predicted by the finite element model for elastic behavior (black) and viscoelastic behavior (gray). In the first 15 minutes, the thermo-elastic response is the same for both models, the plate's deflection evolution is governed by the differences in the coefficient of thermal expansion between the reinforcement plies. Once the isotherm is reached after 15 minutes, the plates deflection obtained with the elastic model remain constant through the time. However, the deflection of the plate obtained with the simulation carried out with the viscoelastic model increases with the time, as it was experimentally observed.

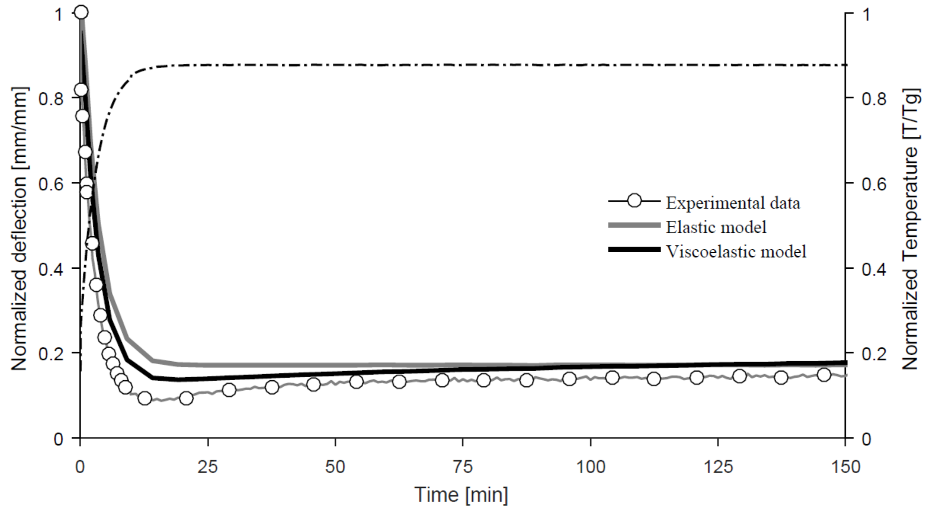

Figure 4-3. Experimental and numerical comparison of the plates maximum deflection during a 150 minutes isotherm at T=Tg-20°C

Finally, Figure 4-4 compares the maximum plate deflection after manufacturing obtained experimentally versus the numerical calculation. The experimental observations indicates that the plates presented an increment of 11% of the total deflection after having set to a 150 minutes isotherm (creep behavior). The numerical simulation with the elastic model do not take this phenomena into account, thus resulting both calculation in the same deformation. The viscoelastic simulation, however, did predict this differential behavior of the composite at high temperature.

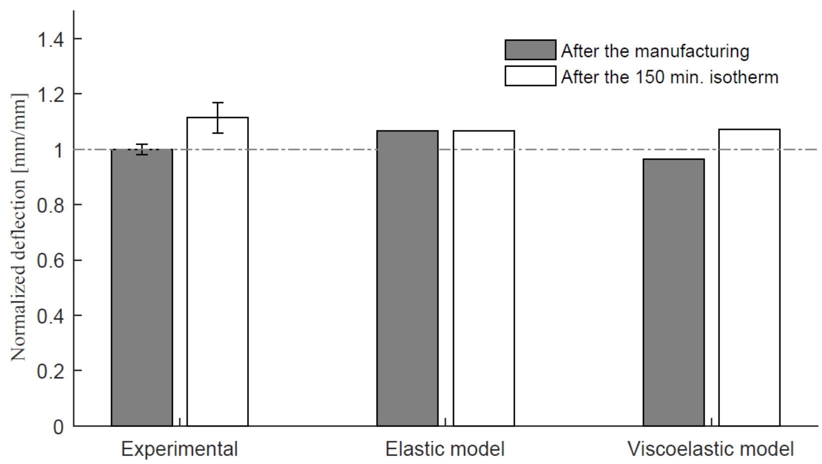

Figure 4-4. Maximal plate deflection at room temperature after the manufacturing (gray) and after the 150 minute isotherm.

5 CONCLUSION

In this study, a digital image analysis was used to measure the geometrical instabilities of asymmetric plates reinforced with 3D interlock fabric. The plate's curvature were characterized after the manufacturing and during a 150 minutes isotherm.

A finite element solution was implemented to simulate the geometrical instabilities caused by residual stresses generation during the reheating and cool-down of the plates. A comparison between the elastic and viscoelastic behavior has been presented. Both models presented good agreement with the plate's deflection measured at room temperature after the manufacturing (i.e. prior to reheating).

The impact of the viscoelastic creep behavior in the geometrical instability was observed while heating the plates at temperatures near the resin glass transition temperature for 150 minutes. Experimentally, an increment of 11% of the total deflection at room temperature was accounted after reheating and cooling-down. Numerically, the viscoelastic model follows the same tendency as the experimental observations. The elastic model did not predict the creep phenomena during the isotherm resulting in accurate deformations.

The presented results suggest that a thermo-viscoelastic model is required to accurately predict the residual stresses generation and geometrical instability during the composite manufacturing of these 3D woven fabrics.

6 ACKNOWLEDGMENT

The authors would like to acknowledge Safran Group and the Canada Research Chair program for the financial support and for providing the resin and reinforcements used in this work. The National Science and Engineering Research Council (NSERC) of Canada, the Fonds Québécois pour la Recherche sur la Nature et les Technologies (FQRNT), the Canada Foundation for Innovation (CFI) and of the Ministère de l'Éducation du Québec are gratefully acknowledge for their contribution with the infrastructure and expenses of the composite laboratory.

7 REFERENCES

1. Mouritz, A.P., et al., *Review of applications for advanced three-dimensional fibre textile composites.* Composites Part A: Applied Science and Manufacturing, 1999. **30**(12): p. 1445-1461.
2. Liu, Y., M. de Araujo, and H. Hu, *2 - Advanced fibrous architectures for composites in aerospace engineering*, in *Advanced Composite Materials for Aerospace Engineering*2016, Woodhead Publishing. p. 17-58.
3. Bersee, H.E.N., P.P. Parlevliet, and A. Beukers, *Residual stresses in thermoplastic composites-A study of the literature-Part I: Formation of residual stresses.* Composites Part A (Applied Science and Manufacturing), 2006. **37**(11): p. 1847-57.
4. Svanberg, J.M. and J.A. Holmberg, *An experimental investigation on mechanisms for manufacturing induced shape distortions in homogeneous and balanced laminates.* Composites Part A (Applied Science and Manufacturing), 2001. **32A**(6): p. 827-38.
5. Radford, D.W. and T.S. Rennick, *Separating Sources of Manufacturing Distortion in Laminated Composites.* Journal of Reinforced Plastics and Composites, 2000. **19**(8): p. 621-641.
6. Ruiz, E. and F. Trochu, *Numerical analysis of cure temperature and internal stresses in thin and thick RTM parts.* Composites Part A (Applied Science and Manufacturing), 2005. **36**(6): p. 806-26.
7. Canal, L.P., et al., *Process-induced strains in RTM processing of polyurethane/carbon composites.* Composites Part A: Applied Science and Manufacturing, 2015. **78**: p. 264-273.

8. Khoun, L., et al., *Investigation of process-induced strains development by fibre Bragg grating sensors in resin transfer moulded composites.* Composites Part A: Applied Science and Manufacturing, 2011. **42**(3): p. 274-282.
9. Garstka, T., et al., *In situ measurements of through-the-thickness strains during processing of AS4/8552 composite.* Composites Part A, 2007. **38**(12): p. 2517-26.
10. Causse, P., E. Ruiz, and F. Trochu, *Experimental study of flexible injection to manufacture parts of strong curvature.* Polymer Composites, 2011. **32**(6): p. 882-895.
11. Palerosi, A.C. and S.F.M. de Almeida, *Thermoelastic evaluation of composite laminates using digital imaging processing.* Composites Part A: Applied Science and Manufacturing, 2007. **38**(11): p. 2283-2293.
12. Kominar, V., *Thermo-mechanical regulation of residual stresses in polymers and polymer composites.* Journal of composite materials, 1996. **30**(3): p. 406-415.
13. Pupin, C., et al., *Formation and suppression of volatile-induced porosities in an RTM epoxy resin.* Composites Part A: Applied Science and Manufacturing, 2017. **94**: p. 146-157.
14. Courtois, A., Hirsekorn, M., Vernet, N., Marcin, L., Ruiz, E., Levesque, M. , *Viscoelastic behavior of an epoxy resin during cure: Characterization and modeling*, in *The 10th International Conference on the Mechanics of Time Dependent Materials*2016: Paris.
15. Machado, M., et al., *Thermomechanical viscoelastic analysis of woven-reinforced thermoplastic-matrix composites.* Composite Structures, 2016. **157**: p. 256-264.